PHILOSOPHICAL TRANSACTIONS OF THE ROYAL SOCIETY A
MATHEMATICAL, PHYSICAL & ENGINEERING SCIENCES

Reduction and Prediction of Sandstone Reservoir Potential, Jurassic, North Sea [and Discussion]

J. G. Gluyas, B. Spiro, R. Raiswell, R. A. Berner, Caroline J. Lowrey, M. L. Coleman, R. Mason, J. H. McD. Whitaker, G. C. Saigal and C. D. Curtis

Phil. Trans. R. Soc. Lond. A 1985 **315**, 187-202
doi: 10.1098/rsta.1985.0036

Phil. Trans. R. Soc. Lond. A **315**, 187–202 (1985) [187]
Printed in Great Britain

Reduction and prediction of sandstone reservoir potential, Jurassic, North Sea

By J. G. Gluyas[†]

Stratigraphic Laboratory, BP Petroleum Development (NWE) Ltd, Dyce, Aberdeen AB2 0PB, U.K.

Porosity, permeability, mineralogical and depth data for two North Sea Jurassic sandstone sequences were analysed. Both sequences show statistically significant negative correlations between present burial depth and porosity. The influence of secondary porosity creation is subordinate to that of the general decline in porosity. For a given burial depth, sequence A is, on average, a little more porous (about 3 %) than B. However, for a given porosity sequence A displays a permeability 1–3 orders of magnitude greater than B.

The large permeability difference between A and B is a function of authigenic mineralogy. The only significant cement within the reservoir intervals of sequence A is quartz. Sequence B contains authigenic clays, quartz and subordinate carbonate. The abundant authigenic clay in B severely reduced permeability.

In both instances, the cements are products of burial and were precipitated from pore waters expelled from shales during compaction. The expelled pore waters were both acidic and rich in solutes; a product of reactions between maturing organic matter, clays and iron oxides. The difference in authigenic mineralogy between the sequences was caused by the reaction between pore waters and sandstones with different detrital mineral compositions. Thus the present reservoir quality is a product of burial and of the reactions between evolving pore fluids and minerals in the sandstone.

INTRODUCTION

Time and money in hydrocarbon exploration can be optimized if the geologist understands and can predict the porosity and permeability characteristics of a reservoir. The aim of this study is to investigate how the porosity–depth and porosity–permeability relations vary and how they developed.

Two Jurassic sandstone sequences (A and B) have been studied. Both display negative correlations between porosity and depth. At typical reservoir depths (3–5 km), sequence A is a few percent more porous than B although it displays permeabilities 1–3 orders of magnitude greater than B. Sequence A forms a single reservoir unit while sequence B is divisible into three reservoir units. These will be referred to as B.1, B.2 and B.3. The three units differ slightly in their environment of deposition, petrography and, possibly, provenance. The porosity and permeability data are from conventional core analysis; about 600 pairs of analyses were used in the study. The descriptions and interpretations are based upon point-count analysis of about 170 thin sections. Many samples were also examined by using a scanning electron microscope.

The evolution of reservoir characteristics is interpreted in terms of mineralogical changes in the sandstones from deposition to the present day. These changes result from diagenetic processes which occurred both within the sandstones and adjacent shales.

[†] Present address: Sedimentology Branch, BP Petroleum Development Ltd, Britannic House, Moor Lane, London EC2Y 9BU, U.K.

Porosity–depth relations

Introduction

Sandstones that would have formed good reservoirs at deposition were investigated; samples rich in matrix clay were excluded from the study. In addition, both sequences studied have short (0.5–2 m) intervals which are completely carbonate cemented. Although excluded from the porosity–depth plots these intervals were considered in the remainder of the study, because carbonate cementation was an important event.

Method and results

Regression analysis was used to quantify changes in porosity as a function of burial depth. A straight-line equation was fitted to each data set. In all four cases (sequence A and sequence B, parts B.1, B.2 and B.3) the correlation coefficients for the porosity–depth equations have high significance values (greater than 99.9%, table 1).

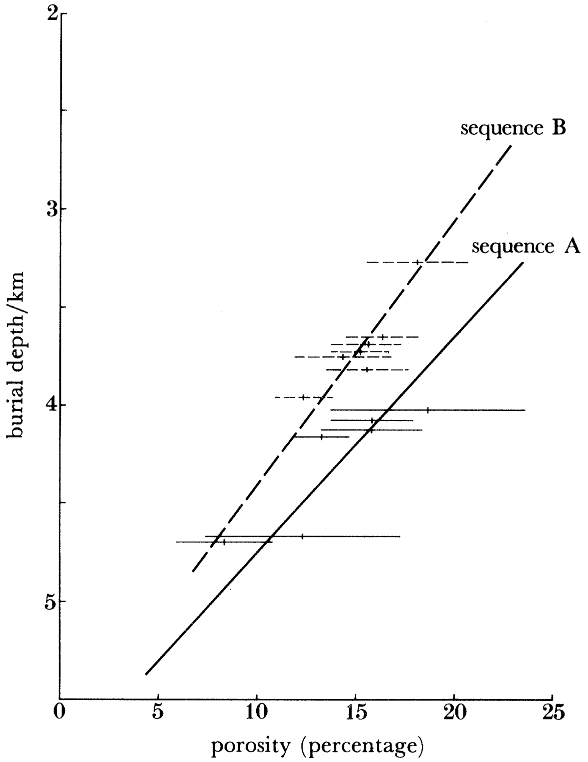

Figure 1. Porosity–depth plot for sandstones from Jurassic sequences A and B. Error bars are ±1 standard deviation. Total number of sample pairs is 636.

Table 1. Regression equations for porosity–depth analysis

sequence	intercept, i	gradient, g	regression coefficient	number of samples	significance (percentage)
A	52.8	−9.0	−0.51	219	> 99.9
B.1	42.3	−7.3	−0.41	159	> 99.9
B.2	42.6	−7.0	−0.51	173	> 99.9
B.3	42.2	−7.2	−0.40	85	> 99.9

Equations are in the form $\phi = gx+i$, where ϕ = porosity and x = depth.

Both sequences display an overall decline in porosity with increased burial depth (cf. Selley 1978; Hayes 1979). The regression equations for the three parts of sequence B are about the same (figure 1). Although the porosity variation at any given depth is large, the average porosity trends can be precisely defined. Thus, provided that oil migrated into a reservoir after burial to its present depth, the average porosity can be defined at any given depth. It is therefore possible to calculate a 'cut-off' depth at which a reservoir becomes an uneconomic exploration target. By taking an arbitrary figure of 10% porosity this depth is shown to be 4800 m in sequence A and 4400 m in sequence B.

POROSITY–PERMEABILITY RELATIONS

Introduction

The same samples were used for both porosity–depth and porosity–permeability analysis. Regression analysis was performed between porosity and the logarithm of the permeability. Straight-line equations were fitted to the data (figure 2; table 2).

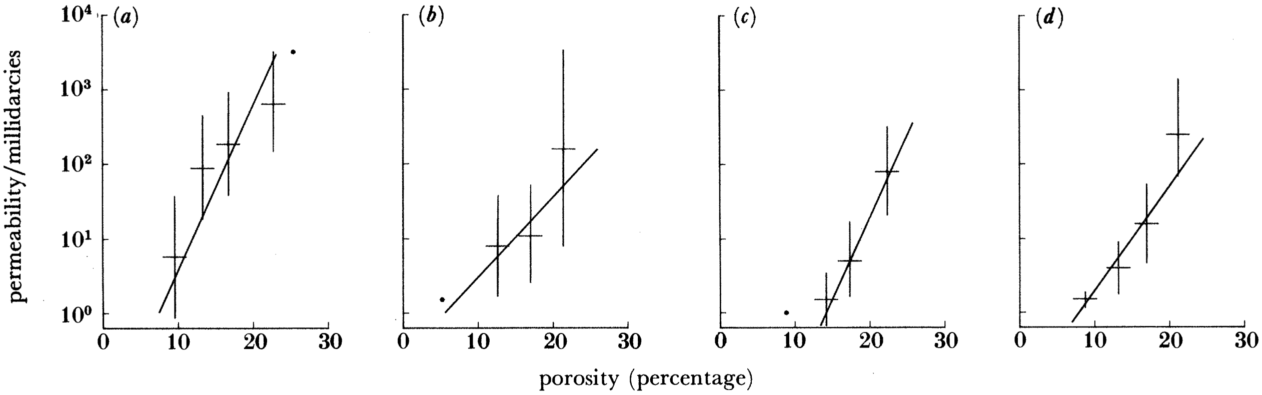

FIGURE 2. Porosity–permeability plots for sandstone from Jurassic sequences A and B. Data averaged within 5% porosity intervals. Error bars are ±1 standard deviation. (*a*) Sequence A; (*b*) sequence B.3; (*c*) sequence B.2; (*d*) sequence B.1. (1 darcy = 9.86923×10^{-1} μm^2.)

TABLE 2. REGRESSION EQUATIONS FOR POROSITY–PERMEABILITY ANALYSIS

sequence	intercept, *i*	gradient, *g*	regression coefficient	number of samples	significance (percentage)
A	−1.24	0.20	0.52	219	> 99.9
B.1	−1.07	0.14	0.75	159	> 99.9
B.2	−3.07	0.22	0.85	173	> 99.9
B.3	−0.62	0.11	0.40	85	> 99.9

Equation is of the form $\lg k = \phi x + i$, where k = permeability and $\phi = gx + i$ = porosity.

Results

All four calculated porosity–permeability equations are different and all have high significances (table 2). In general, irrespective of porosity, sequence A is much more permeable than sequence B. Similarly, the permeability of B.2 is less than that of the other parts of sequence B and sequence A (figure 2). Again, the trends shown are averages and, although for a given porosity the variations in permeability are large, the average values can be precisely defined.

It is now possible to use economic criteria to define minimum permeability requirements. If 10 mD is chosen as an arbitrary figure, then the required porosities to achieve such a permeability are A = 11, B.1 = 15, B.2 = 18.5 and B.3 = 15%. These porosity figures in turn allow the economic limit of burial depth to be revised, giving A = 4.6, B.1 = 3.7, B.2 = 3.4 and B.3 = 3.8 km.

FACTORS CONTROLLING POROSITY AND PERMEABILITY

The main factor controlling the decline in porosity from the most shallow to the deepest samples is increased cementation. It is difficult to prove positively the above statement because of the variability in the cement content of the samples. However, in both sequences, compaction occurred during relatively early stages of diagenesis and stopped before the major cementation and dissolution events. Compaction cannot be used to explain the porosity–depth trends. It is significant that although dissolution events (that is, creation of secondary porosity) are recognized in both sequences, they did not halt the overall trend of porosity reduction with depth.

Permeability is highly sensitive to the morphology and location of authigenic cements within pore spaces. Clay minerals that have small crystal sizes and large surface area:volume ratios reduce permeability dramatically. Conversely, quartz and carbonate cements have small surface area:volume ratios and although locally cementation may reduce porosity to very low values, the bulk effect upon reservoir permeability is far less than that of equivalent volumes of authigenic clay.

Both the quantity and type of clay mineral precipitated govern the response of permeability to cementation. Sequence A sandstones contain little authigenic clay and commonly display high permeability. The sandstones of sequence B contain up to 25% clay cement, consisting mainly of kaolinite and illite. The filamentous illite reduces permeability more drastically than the tabular kaolinite crystals (table 3; Stalder 1973).

The remainder of this study investigates the origin of the cements and thus the ultimate controls on reservoir porosity and permeability.

DIAGENESIS OF SEQUENCE A

Description

Sequence A sandstones have a simple diagenetic history (figure 3). Calcite nodules formed during the earliest stages of diagenesis. Both ferroan and non-ferroan calcites occur and the nodules commonly contain about 1% by volume of pyrite. They are approximately spherical and range in size from 0.05–2 m. The nodules contain about 35% by volume of cement (carbonate and pyrite), about 65% by volume of fabric grains and no visible porosity (less than 5% measured porosity. Visible porosity is that which can be seen and point-counted by using thin-section petrography. Measured porosity is obtained from conventional core analysis). The cement precipitated passively against the quartz and feldspar with no evidence of fabric grain replacement.

Quartz cementation followed that of carbonate. Most quartz grains which were not already cemented by calcite developed euhedral quartz overgrowths, differentiated from the host grain by a 'dust rim'. The authigenic quartz comprises 5.7 ± 3.1% by volume of the rock (75 samples;

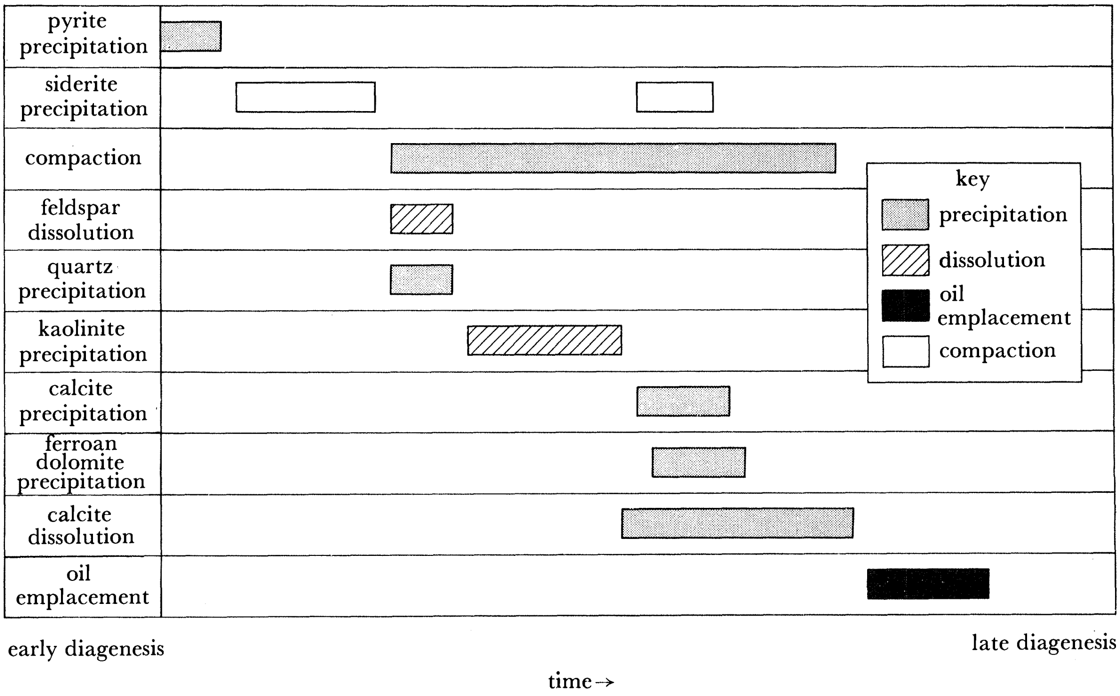

FIGURE 3. Diagenetic history of sequence A sandstones.

table 3). Almost all of the remaining solid rock (90–100 %) is composed of detrital grains. Visible and measured porosities lie between 10 and 25 % with an average visible porosity of 12 %.

Minor feldspar leaching and associated kaolinite precipitation occurred at about the same time as quartz precipitation. Although individual feldspars are extensively leached the event is of minor volumetric importance because the sediment at deposition, now preserved in the nodules, contained few detrital feldspars. Similarly, kaolinite is often absent and, where present, rarely exceeds 0.5 % by volume.

TABLE 3. MINERALOGICAL COMPOSITION OF THE STUDIED SANDSTONES

	no.	qtzd	feld	mica	other	mtx	org	carb	sid	qtzc	pyt	kao	ill
					mean mineralogical composition (percentage by volume)								
A′	12	57.5	3.1	0.4	0.6	0.0	0.4	37.3	0.0	0.0	0.4	0.0	0.3
A″	56	86.3	2.0	1.0	1.6	0.9	1.1	0.2	0.0	5.3	0.2	0.1	1.3
B.3	42	77.7	0.8	1.5	0.5	2.1	0.3	1.3	0.8	5.8	0.5	5.6	3.1
B.2	18	74.1	3.3	1.9	1.1	1.2	0.4	1.8	0.0	3.9	0.4	6.1	5.8
B.1	28	60.6	1.6	0.9	1.5	0.1	0.6	10.8	2.1	6.7	0.5	11.2	3.4
						standard deviation							
A′	12	2.0	0.6	0.2	0.0	0.1	0.7	4.0	0.0	0.0	0.3	0.0	0.1
A″	56	4.2	0.9	0.5	0.6	0.6	0.8	0.2	0.0	1.6	0.1	0.0	0.9
B.3	42	10.3	0.9	2.3	0.6	3.0	0.6	6.5	2.1	4.1	1.3	5.7	2.5
B.2	18	7.1	1.8	1.7	1.5	1.3	0.6	7.3	0.0	3.8	0.6	3.2	3.8
B.1	28	9.2	1.5	1.4	1.6	0.3	1.0	14.8	4.6	4.6	2.1	6.2	2.6

Where no. = number of samples, qtzd = detrital quartz, feld = feldspar, mica = mica, other = other fabric grains, mtx = matrix clay, carb = calcite and dolomite (ferroan and non-ferroan), sid = siderite, qtzc = quartz cement, pyt = pyrite, kao = kaolinite, ill = illite. A′ = carbonate-cemented, A″ = quartz-cemented.

During the latter stages of quartz precipitation carbonate leaching began. Many of the calcite nodules have digitate margins and partly decalcified rims. Unlike the 'fresh' feldspars in the nodules, feldspars in the rims are commonly leached. Few quartz grains in the rims have authigenic quartz overgrowths and some grains have sutured (stylolitized) grain contacts.

In the quartz-cemented intervals there are patches of late diagenetic ferroan calcite (about 10 cm in diameter). This calcite differs from that forming the nodules. Its precipitation post-dated that of quartz. It has a patchy, diffuse distribution and, unlike the nodular carbonate, lacks mineral fluorescence under ultraviolet light.

The deeper intervals (at 4.7 km) do not contain late-diagenetic calcite, although most samples have trace quantities of late-diagenetic ferroan dolomite. This carbonate occurs as euhedral crystals 50–100 μm in diameter. It precipitated both with primary pore spaces and replaced relict detrital feldspar. Authigenic illite was precipitated at about the same time as the late-diagenetic carbonate. It usually occurs in isolated patches (about 300 μm in diameter), where it both replaces and has nucleated on detrital clay clasts. After illite precipitation, oil migrated into the reservoir.

Interpretation

The spherical calcite and pyrite nodules are typical by-products of early diagenetic bacterial activity in marine sediments. The nodules were formed near to the sediment–water interface via sulphate reduction and concomitant organic matter oxidation (Irwin & Hurst 1983; Gluyas 1984). Sulphide released by the sulphate reduction reacted with iron and precipitated as pyrite (Raiswell & Plant 1980). The bicarbonate reacted with the pore waters to precipitate as calcite (Raiswell 1976).

The porosity of the sediment before calcite precipitation was about 40% by volume. This figure is calculated from addition of the present porosity and the volume of carbonate cement. A porosity of 40% by volume is about that of an unconsolidated sand (Pettijohn 1975). Thus the nodules grew before much sediment compaction had occurred.

Quartz cementation is usually attributed to one or more of three processes.

(i) Dissolution of feldspar *in situ* to produce quartz and kaolinite (Hurst & Irwin 1982).

(ii) Compaction-driven expulsion of $Si(OH)_4^0$-charged waters from adjacent shales. The $Si(OH)_4^0$ is produced during clay mineral transformations (Boles 1981).

(iii) Pressure dissolution of quartz grains within the sandstones producing dissolved silica that may subsequently precipitate as a cement. The dissolution may partly affect all grains (penetrative) or may result in stylolite formation (non-penetrative).

Which of these processes operated to cement and reduce porosity in sequence A?

Feldspar is not and never was present in sufficient quantity to supply the volume of quartz cement recorded. The sandstones now contain about 2% by volume feldspar. Point-count data from calcite nodules suggest that at deposition the sandstones contained up to 5% by volume of feldspar. Diagenetic dissolution of this component has produced some kaolinite and, probably, some quartz. However, the proportion of quartz cement that could have been produced in this way was of minor importance.

If all of the quartz cement was derived externally (from shales) or from stylolitization then the sum of the quartz cement percentage by volume, Q, and the visible porosity, V, should be equal to the original porosity. The studied samples have an average visible porosity of about 12%. The same (75) samples have an average quartz-cement content of $5.7 \pm 3.1\%$. The precision on point counting such an amount is ±4% (Pettijohn *et al.* 1973). At the most extreme range of error this gives a maximum quartz cement content of about 13%. Thus the maximum value of $Q+V = 25\%$. The porosity is 15% less than that quoted for unconsolidated medium-grained sand (Pettijohn 1975) and 12% less than the 'minus cement' porosity of the carbonate nodules.

The discrepancy of 12–15% between the calculated porosity (25%) and the porosity at deposition (40%) must be the product of compaction-induced (penetrative) dissolution and grain rearrangement (Füchtbauer 1967). By using Füchtbauer's (1967) calculations a 28% loss in porosity (from 40 to 12%), resulting from grain rearrangement and penetrative pressure dissolution would require only 0.6% by mass of the sandstone to dissolve and reprecipitate. Thus, although penetrative grain dissolution could account for the observed loss in porosity it could not have provided the observed quantity of cement. In contrast, if the authigenic quartz was derived from adjacent shales, we can account for the quartz-cement content but only half the porosity loss. Therefore the decline in porosity from deposition to the present day must result from a combination of grain rearrangement (compaction) and quartz cement precipitation. Both processes produced a porosity loss of between 10 and 15%. There is no evidence of quartz grain dissolution after quartz cementation, therefore the compaction must have occurred before cementation.

That feldspar and carbonate leaching occurred at the same time as quartz precipitation indicates that not only were the pore waters saturated with silica but also acidic. Both dissolution reactions consume acid (Krauskopf 1979), i.e.

$$\mathrm{H^{+}+HCO_3^{-}+CaCO_3 \rightleftharpoons Ca^{2+}+2HCO_3^{-}} \quad \text{(carbonate dissolution)}, \tag{1}$$

and

$$\mathrm{2H^{+}+2HCO_3^{-}+KAl\,Si_3O_8+6H_2O \rightleftharpoons 3Si(OH)_4^{0}+K^{+}+Al(OH)_2^{+}+2HCO_3^{-}} \quad \text{(feldspar dissolution)}. \tag{2}$$

Although this acid could not have originated within the sandstone it could have been generated within shales. The major acid source is from decarboxylation of organic matter (Schmidt & McDonald 1979; Carothers & Kharaka 1980). The acids are carbon based and comprise carbonic acid or simple organic acids or both. In addition, smectite to illite transformations may also produce acid (Hower 1981). As sequence A is located close to its (oil) source rock the major influences on sandstone diagenesis were almost certainly organic matter maturation and clay mineral transformation. During organic matter maturation the light acid radicals are released just before oil generation occurs. It is significant therefore that petrographic evidence suggests that the leaching described occurred just before oil was emplaced in the reservoir.

DIAGENESIS OF SEQUENCE B

Description

The diagenetic history of sequence B sandstones is more complicated than that of sequence A (figure 4). Small quantities (about 1% by volume) of siderite and pyrite were precipitated during the earliest stages of diagenesis. Although pyrite and siderite may occur in the same sample they are never directly juxtaposed on a microscopic scale.

The bulk of compaction and grain rearrangement occurred in the interval between earliest

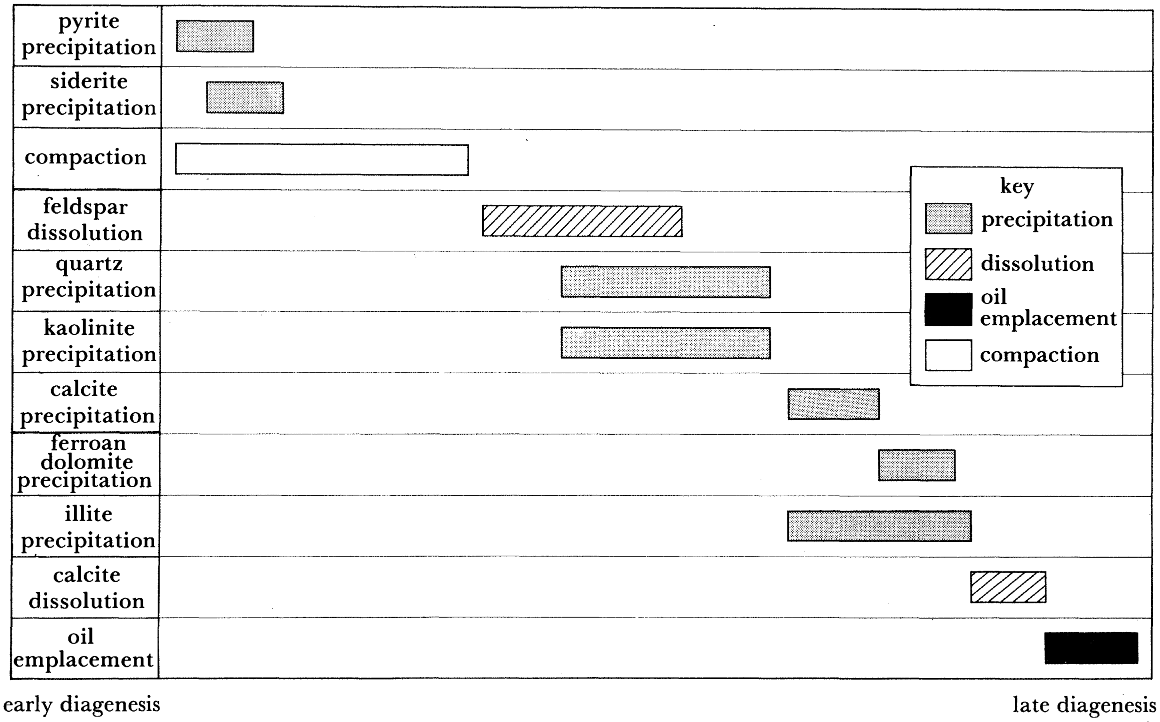

FIGURE 4. Diagenetic history of sequence B sandstones.

diagenesis and subsequent diagenetic (chemical) events. Detrital mica grains were deformed around quartz grains and clay clasts squashed to form pseudomatrix.

As discussed above, the porosity loss caused by compaction may be calculated by adding the present porosity and the authigenic mineral content and subtracting porosity created by mineral dissolution. Thus the average porosity of sequence B sandstones after compaction was 30 ± 5 % by volume. That is to say, compaction reduced the porosity by about 10 % by volume (assuming an average value of about 40 % porosity for unconsolidated sand (Pettijohn 1975).

After compaction, feldspar dissolution began, followed shortly by quartz and kaolinite precipitation. All three processes appear to have overlapped in time and space. The present feldspar content is 1–3 % by volume. Most feldspar grains suffered at least partial dissolution. In some instances 'clay rim' pores testify to the former presence of (?) feldspar grains. Summation of these 'clay rims' pores and evidence from clay-rich diagenetically immature portions of the sandstones suggests that the sandstones now contain between 25 % (unit B.3) and 60 % (unit B.1) of the feldspar they did at deposition.

Clusters of kaolinite platelets occur throughout the sandstones. Individual crystals are commonly 10 μm in diameter. Intertwined vermicules of stacked crystals fill both primary depositional pore spaces and secondary pores within partly dissolved feldspars. Authigenic quartz occurs as syntaxial overgrowths on detrital grains; most bear overgrowths. Quartz and kaolinite cements are commonly juxtaposed; their precipitation was probably synchronous.

Large poikilotopic crystals of calcite developed after the phase of feldspar dissolution and quartz and kaolinite precipitation (figure 4). Although the calcite precipitated passively against quartz overgrowths it replaced some kaolinite. Such poikilotopic calcite is only abundant in unit B.1 (10 ± 15% by volume). Subsequent precipitation of ferroan dolomite replaced not only clays but also quartz, feldspar and calcite. It occurs as rare small (8 μm) crystals in unit B.3. In the two deepest wells it occurs as large poikilotopic crystals in unit B.1. Some of the calcite crystals appear to have suffered partial dissolution as many have highly digitate margins and scattered patches are often in optical continuity.

Precipitation of authigenic illite was apparently synchronous with carbonate. The clay occurs mostly as elongate, pore-filling, fibres which project from detrital clots of illitic matrix clay and the edges of kaolinite crystals.

Finally, oil entered the sandstones and effectively halted diagenesis.

Interpretation

The early diagenetic iron materials siderite and pyrite are products of bacterial metabolism (Curtis *et al.* 1972; Berner 1970). Both develop in reducing conditions caused by organic matter oxidation. The sulphide in pyrite was derived from reduction of sulphate, which was readily available in sea water. In contrast, siderite only precipitated when sulphide activity was low. It thus tended, during early burial, to form from non-marine pore solutions. The distributions of pyrite and siderite within the different parts of sequence B are compatible with the varied early diagenetic pore-fluid compositions deduced from the analysis of sedimentological facies.

The processes of feldspar dissolution and quartz and kaolinite precipitation are similar to those that occurred in sequence A. However, the quantities and proportions of the minerals precipitated and dissolved are very different (table 3).

Possible origins of quartz cement for sequence A are (i) feldspar dissolution, (ii) clay transformations in associated shales, (iii) pressure dissolution of quartz grains. Of these, feldspar dissolution and clay transformation can also induce kaolinite precipitation. Because the original feldspar content has been deduced, the approximate maximum contribution of *in situ* feldspar grain dissolution to the kaolinite and quartz cement contents is easily calculated. Equation (2) may be rewritten to give aluminium as a solid (kaolinite) rather than dissolved element, i.e.

$$2H^+ + 2HCO_3^- + \underset{\text{(orthoclase)}}{2KAlSi_3O_8} + H_2O \rightleftharpoons 2HCO_3^- + \underset{\text{(kaolinite)}}{Al_2Si_2O_5(OH)_4} + 4SiO_2 + 2K^+. \quad (3)$$

Note again the presence of H^+ (acid) in the reactants. The only difference between the products of reactions (2) and (3) is in the implied position of equilibrium in the quartz and kaolinite precipitation–dissolution reactions (Curtis 1983; Hazeldine *et al.* 1984).

If the kaolinite and quartz precipitation reactions were able to attain the thermodynamic impossibility of 100% efficiency, the summed volumes of kaolinite and quartz cements would equal the volume of (potassium) feldspar dissolved. This is because the densities of the three minerals are about the same and the atomic mass of the precipitated products is only a little less than that of the solid reactants (potassium is lost to solution). In fact the quantity of kaolinite and quartz cement precipitated is between 5 and 10 times greater than that which could have been supplied by dissolution of detrital grains within the sandstones (table 3). Therefore most of the elements forming the kaolinite and quartz cements must have been supplied from an external source.

The most probable source of the necessary elements is from reactions in and subsequent dewatering of shale (Curtis 1983). Sequence B is encased in and interbedded with shale. It is also (now) filled with oil generated within more distant and structurally deeper shale. It is thus certain that shale-derived connate water passed through the sandstones of sequence B.

Dissolved aluminium and silicon required for kaolinite and quartz precipitation may be generated via dissolution of detrital micas and feldspars in shales. The driving force behind the dissolution reactions is acid generation caused by organic matter maturation, smectite to illite transformations or both (Hower 1981; Curtis 1983). The fact that feldspar dissolution occurred in the sandstones of sequence B indicates that the shales released acidic pore waters. Dissolution of detrital feldspar in the sandstones may have been sufficient to increase pH and dissolved aluminium concentration and push the pore water composition into the kaolinite stability field (figure 5). Silica also precipitated as authigenic rims on quartz grains.

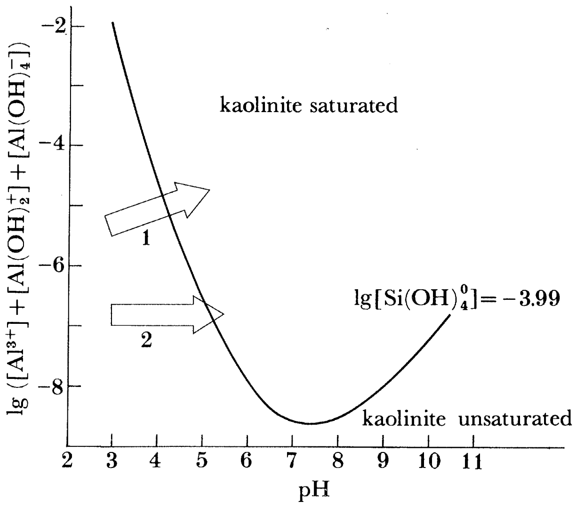

FIGURE 5. Stability field of kaolinite relative to dissolved species of silicon and aluminium. Pore-fluid evolution on entering sequence B = 1, and for sequence A = 2. Modified from Curtis (1983).

The implication that acid generation in adjacent or more distant source-shale controlled diagenesis has an important consequence. A charge balance must be maintained in the solution. Therefore for hydrogen ions (acid) to be transported in solution at low pH an acid anion is required. At diagenetic temperatures the only suitable proton donor in systems closed to oxidants is bicarbonate (Curtis 1983). This has been recorded in oilfield brines where it is believed to have been derived via decarboxylation in hydrocarbon source rocks (Carothers & Kharaka 1980). Thus bicarbonate has been added to both sides of the equations presented earlier to maintain charge balance with a 'sensible' acid anion.

The presence of bicarbonate in a system where acid is being consumed is likely to lead to carbonate precipitation, i.e.

$$M^{2+} + 2HCO_3^- \rightleftharpoons MCO_3 + H^+ + HCO_3^-, \qquad (4)$$

where $M = Ca, Mg, Fe.$

Sequence B contains authigenic carbonate, which precipitated after quartz and kaolinite. In the absence of stable-isotope (C and O) analysis, proof that the carbonate is a product of source rock decarboxylation is lacking. However, similar late-diagenetic carbonate cements in other sandstones have given stable-isotope signatures interpreted as decarboxylation products and precipitated at a depth of a few kilometres (Irwin & Hurst 1983).

Precipitation of illite, which was roughly synchronous with precipitation of carbonate, can be interpreted in terms of temperature and relative potassium and hydrogen ion activities (lg (a_{K^+}/a_{H^+}); see Hutcheon 1981 and figure 6). Precipitation of illite occurred later and thus deeper and at higher temperatures than that of kaolinite. This is to be expected from the phase relations (figure 6).

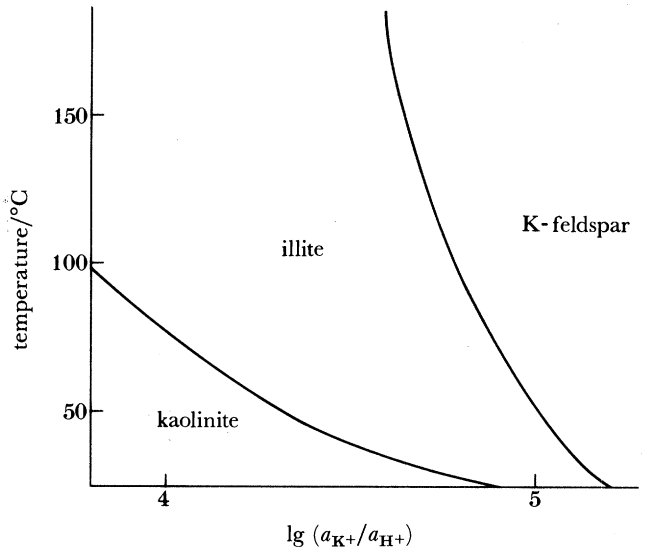

FIGURE 6. Phase relations within the system kaolinite–illite–K-feldspar (from Hutcheon 1981). (Pressure = 500 bar; 1 bar = 10^5 Pa.)

It is difficult to determine the likely $K^+ : H^+$ ratio of the pore solutions. This is because in the shales acid was generated from organic matter maturation and smectite–illite transformations. Potassium was generated during detrital mineral dissolution; a process that consumes acid, whereas the clay mineral transformation consumes potassium. However, the fact that the solutions left the shales while at an acidic pH is demonstrated by the presence of partly dissolved feldspars. On leaving the shales there was no balance of reactions, acid was consumed and potassium generated as feldspars and other minerals dissolved. These reactions continued in the reservoir sandstones.

The eventual depletion of H^+ in the pore waters is indicated by the presence of carbonate. The fact that the last-formed diagenetic carbonates are iron-rich implies that solid ferric oxides were dissolved and reduced (Berner 1971); this process results in a massive pH increase (Irwin 1980);

$$\underset{\text{(organic matter)}}{(CH_2O)} + 4FeOOH + H_2O \rightleftharpoons 4Fe^{2+} + HCO_3^- + 7OH^-. \qquad (5)$$

As hydroxide is a powerful proton acceptor it would have produced an increase in the lg (a_{K^+}/a_{H^+}) ratio, favouring illite precipitation (figure 6).

Finally, a return to acidic pore waters resulted in the dissolution of some of the late-diagenetic carbonate. This too was probably associated with organic matter maturation because after this, oil migrated into the reservoir.

Synthesis

Both of the sandstone sequences studied have diagenetic histories that were controlled by organic matter maturation and clay transformations in oil source rock shales. Despite the fact the reservoirs share a common source rock, diagenesis has produced reservoirs of vastly different quality. The question, 'what has caused this difference?' is addressed below.

The sandstones differ in their environment of deposition, initial sandstone composition and distance from their oil source rock (table 4).

TABLE 4. ENVIRONMENT OF DEPOSITION, COMPOSITION AND DISTANCE FROM OIL SOURCE OF THE TWO SANDSTONE SEQUENCES

sequence	environment of deposition	fabric grain composition	distance from oil source rock
A	marine	$> 95\%$ quartz $< 5\%$ mica, feldspar etc.	adjacent to source rock
B	marginal marine	$< 95\%$ quartz $> 5\%$ mica, feldspar etc.	separated from source rock by thick shale

The environment of deposition influenced earliest diagenesis, with the production of calcite nodules in the marine sandstones of sequence A and pyrite and siderite in the marginal marine sandstones of sequence B. All three minerals are products of bacterial processes that operate only at shallow burial depths.

It is probable that the differences in detrital mineralogy influenced the later stages of diagenesis. The relatively feldspathic sequence B sandstones may have caused the pore water expelled from the shales to increase in pH and precipitate their dissolved aluminium load in the form of authigenic clays (kaolinite and illite). In contrast, sequence A sandstones contained little feldspar and the waters expelled from the source rock shales could have passed through with only minor modification to pH and dissolved aluminium content.

Direct evidence of the role played by detrital mineralogy comes from sequence B. The three parts of sequence B are juxtaposed. They must all therefore have been invaded by the same pore water during the feldspar leaching phase of diagenesis. The sequences have, however, reacted differently as shown by their authigenic mineral contents and bulk reservoir properties (figure 2).

It is probable that a second major influence on authigenic mineralogy is the distance from the source of oil (and therefore acid pore water). As soon as pore waters are expelled from shale, acid is consumed via reactions between the pore water and minerals (feldspar, carbonate, etc.). The greater the distance the pore water travels in sandstone, the more likely it is to have a high pH and high dissolved aluminium content. This means that the probability that it will precipitate clays and carbonate increases with migration distance. As sequence A is adjacent to its source rock while sequence B is relatively distant the high authigenic clay content of sequence B may also be a product of the distance that the shale-derived pore waters travelled.

Conclusions

Both Jurassic sandstone oil reservoir sequences studied display a linear decline in porosity with increased burial depth. Permeability shows a similar but logarithmic, decline.

Both the decline in porosity and permeability result from increased cementation. However, at similar depths the permeability of sequence A is up to three orders of magnitude greater than sequence B. The relatively poor permeability of sequence B is caused mainly by the large quantities of authigenic clay that it contains. Sequence A contains little authigenic clay.

Diagenetic analysis of the two sequences indicates that early diagenesis was controlled by bacterial processes. The bacterial oxidation of organic matter led to locally important cementation by calcite, siderite and pyrite. Thermal processes controlled the subsequent phases of diagenesis. Reactions in shales, between organic matter, clays and iron oxides, produced acidic pore waters rich in dissolved ions. These pore waters, when expelled from the shales, reacted both *en route* to and with the reservoir sandstone to become less acidic and capable of precipitating clay minerals and carbonate.

Sequence A is quartzose and adjacent to its source rock. Reaction between it and water expelled from the source rock was minimal and as such little clay was precipitated. Sequence B is feldspathic and distant from the source rock. This combination resulted in the precipitation of massive quantities of authigenic clay, which dramatically reduced the permeability of the sandstone.

By using the empirically derived depth–porosity–permeability equations it is possible to predict the reservoir quality of the two sequences at any given depth. However, an understanding of the processes that controlled diagenesis and thus reservoir quality, allows not only these two sequences to be successfully modelled but also has greater implications for the potential quality of yet undiscovered reservoirs.

I thank BP Petroleum Development (NWE) Ltd for allowing me to publish this work. I also thank Dr Jon Bellamy for help and encouragement during the study and preparation of the paper.

References

Berner, R. A. 1970 Sedimentary pyrite formation. *Am. J. Sci.* **268**, 1–23.

Berner, R. A. 1971 *Principles of chemical sedimentology*, 240 pp. New York: McGraw-Hill.

Boles, J. R. 1981 Clay diagenesis and effects on sandstone cementation. In *Mineralogical Association of Canada short course in clays and the resource geologist* (ed. F. J. Longstaffe), pp. 148–168. Calgary.

Carothers, W. W. & Kharaka, Y. K. 1980 Stable carbon isotopes of HCO_3^- in oil-field waters – implications for the origin of CO_2. *Geochim. cosmochim. Acta* **44**, 323–332.

Curtis, C. D. 1983 Link between aluminium mobility and destruction of secondary porosity. *Bull. Am. Ass. petrol. Geol.* **67**, 380–384.

Curtis, C. D., Petrowski, C. & Oertel, G. 1972 Stable carbon isotope ratios within carbonate concretions: a clue to time and place of formation. *Nature, Lond.* **235**, 98–100.

Füchtbauer, H. 1967 Influence of different types of diagenesis on sandstone porosity. *Proceedings of the 7th World Petroleum Congress, Mexico*, vol. 2 (ed. W. Ruhl), pp. 353–367.

Gluyas, J. G. 1984 Early carbonate diagenesis within Phanerozoic shales and sandstones of the NW European Shelf. *Clay Miner.* **19**, 309–321.

Hazeldine, R. S. 1984 Quartz diagenesis and convective fluid movement: Beatrice Oilfield, UK North Sea. *Clay Miner.* **19**, 391–402.

Hayes, J. B. 1979 Sandstone diagenesis – the hole truth, *SEPM Spec. Publ.* **26**, 127–139.

Hower, J. 1981 Shale diagenesis. In *Mineralogical Association of Canada short course in clays and the resource geologist* (ed. F. J. Longstaffe), pp. 60–80. Calgary.

Hurst, A. & Irwin, H. 1982 Geological modelling of clay diagenesis in sandstones. *Clay Miner.* **17**, 5–22.
Hutcheon, I. 1981 Applications of thermodynamics to clay minerals and authigenic mineral equilibria. In *Mineralogical Association of Canada short course in clays and the resource geologist* (ed. F. J. Longstaffe) pp. 169–192. Calgary.
Irwin, H. & Hurst, A. 1983 Application of geochemistry to sandstone reservoir studies. *Geol. Soc. Spec. Pub.* Dorset. *Sedimentology* **27**, 577–591.
Irwin, H. & Hurst, A. 1983 Application of geochemistry to sandstone reservoir studies. *Geol. Soc. Spec. Pub* No. 12, pp. 127–146.
Krauskopf, K. B. 1979 *Introduction to geochemistry* (2nd edn), 617 pp. Tokyo: McGraw-Hill.
Pettijohn, F. J. 1975 *Sedimentary rocks* (3rd edn), 628 pp. New York: Harper.
Pettijohn, F. J., Potter, P. E. & Siever, R. 1973 *Sand and sandstone*, 618 pp. New York: Springer-Verlag.
Raiswell, R. W. 1976 The microbiological formation of carbonate concretions in the upper Lias of N.E. England. *Chem. Geol.* **18**, 227–244.
Raiswell, R. W. & Plant, J. 1980 The incorporation of trace elements into pyrite during diagenesis of black shales, Yorkshire, England. *Econ. Geol.* **75**, 684–699.
Schmidt, V. & McDonald, D. A. 1979 The role of secondary porosity in the course of sandstone diagenesis. *SEPM Spec. Publ.* no. 26, pp. 175–207.
Selley, R. C. 1978 Porosity gradients in North Sea oil-bearing sandstones. *J. geol. Soc. Lond.* **135**, 119–132.
Stalder, P. J. 1973 Influence of crystallographic habit and aggregate structure of authigenic clay minerals on sandstone permeability. *Geologie Mijnb.* **52**, 217–220.

Discussion

B. SPIRO (*British Geological Survey, London*). What is the evidence that the rock is flushed by acid before oil emplacement, and is there any evidence that the acids are organic?

J. G. GLUYAS. Petrographic textures indicate that the reservoir was leached before the oil entered. In these sequences there is no direct evidence that the acids were organic, but carbon-based acids (organic or carbonic) are the only ones likely to have been present in sufficient quantity.

R. RAISWELL (*Department of Earth Sciences, Leeds University*). Is it possible that the acid involved is inorganic, rather than organic, and is produced by oxidation of the sulphide minerals? A small amount of sulphide could produce a considerable amount of acid.

J. G. GLUYAS. Both sequences contain early diagenetic sulphide (pyrite). This pyrite does not display any textural evidence that indicates that it has been subject to oxidation and partial dissolution. Additionally, it is difficult to think of an oxidant source in this deeply buried system.

R. A. BERNER (*Department of Geology and Geophysics, Yale University, U.S.A.*). Dr Gluyas has not mentioned the source of the carbonate. Did it come from scattered shells in the original sand?

J. G. GLUYAS. It is probable that shells provided some carbonate during the precipitation of nodular carbonate in sequence A, but much of the carbonate was supplied via bacterial sulphate reduction and concomitant organic matter oxidation. The late-diagenetic carbonate in sequence B was probably derived from organic matter decarboxylation.

R. A. BERNER. If shells were present, there may also have been sponge spicules, which could provide a source for the quartz cement.

J. G. Gluyas. In other sequences rich in spicules at deposition, it is common to find a chert cement with spicule-shaped pores. Such structures are absent in these rocks.

Caroline J. Lowrey (*Department of Geology, Sedimentary Research Laboratory, Reading*). It seems unlikely that biogenic silica could provide a source of silica for the 'late-stage' authigenic quartz described by Dr Gluyas. Biogenic opaline silica is unstable in marine pore waters and would dissolve within a few metres of the sediment–water interface. In any sediment of reasonable porosity and permeability the dissolved silica would then be recirculated into oceanic sea water.

M. L. Coleman (*BP Research Centre, Sunbury-on-Thames*). Dr Gluyas suggested that the carbonate cement originated from sulphate reduction, yet it is cementing a sandstone whose porosity is 35 %. This behaviour does not seem typical for an environment in which sulphate reduction has occurred.

J. G. Gluyas. The sandstones are interbedded with black, bituminous oil shales. It is thus probable that the sandstones were deposited beneath anoxic bottom waters and as such are likely to have undergone a phase of sulphate reduction. Oxidation of organic matter in the sandstones or adjacent shales would have supplied carbonate.

M. L. Coleman. At what depth would the sandstone have a porosity of 35 %?

J. G. Gluyas. Probably within the top 100 m.

R. Mason (*Department of Geology, University College London*). How was the proportion of quartz in overgrowths calculated; by point-counting or by back-calculation from the porosity measurements?

J. G. Gluyas. The porosity measurements are from conventional core analyses. The petrographic information is obtained by point-counting. I also point-counted porosity to discover the proportions of the different pore types. I have also included error estimates in the calculations I described.

J. H. McD. Whitaker (*Department of Geology, The University, Leicester*). In sequence B Dr Gluyas found early trace amounts of siderite and pyrite, but in some parts of this sandstone these minerals are emplaced during a late stage of the diagenesis.

J. G. Gluyas. In the sequences I studied these minerals do not produce an appreciable loss in porosity. They are sometimes trapped beneath earlier diagenetic quartz overgrowths. The late-diagenetic iron minerals tend to be ferroan dolomite and ferroan calcite.

G. C. Saigal (*Department of Geology, St Andrews University, Fife, Scotland*). Was any kaolinite precipitated during the late-stage dissolution of carbonate and feldspars? If it was, then how would Dr Gluyas differentiate between the early- and late-stage kaolinite?

J. G. Gluyas. I did not see any late-stage kaolinite. The reason why I believe that there was a late dissolution event is that some of the patches of carbonate are in optical continuity, even though the grains are now physically separate. But it was probably a minor event.

C. D. Curtis (*Beaumont Building, The University, Sheffield*). Does Dr Gluyas have any traces of late-stage authigenic chlorite and if not, how have the ferroan carbonates been produced?

J. G. Gluyas. These studies were done by using petrographic and mineralogically qualitative techniques. Chlorite is not present in large amounts although small amounts may have been missed. The ferroan carbonates precipitated on the reaction of dissolved iron (from iron oxides) with bicarbonate (released during decarboxylation of organic matter).

J. H. McD. Whitaker. From my own experience only the deeper wells contain appreciable chlorite.

J. G. Gluyas. Dr Whitaker's comment may apply to this sequence, but is not generally true for the North Sea.